

UC Irvine

UC Irvine Previously Published Works

Title

Using nature's blueprint to expand catalysis with Earth-abundant metals

Permalink

<https://escholarship.org/uc/item/3mt2c9pg>

Journal

Science, 369(6505)

ISSN

0036-8075

Authors

Bullock, R Morris
Chen, Jingguang G
Gagliardi, Laura
et al.

Publication Date

2020-08-14

DOI

10.1126/science.abc3183

Peer reviewed



Published in final edited form as:

Science. 2020 August 14; 369(6505): . doi:10.1126/science.abc3183.

Using nature's blueprint to expand catalysis with Earth-abundant metals

R. Morris Bullock^{1,*}, Jingguang G. Chen^{2,3,*}, Laura Gagliardi^{4,*}, Paul J. Chirik⁵, Omar K. Farha⁶, Christopher H. Hendon⁷, Christopher W. Jones⁸, John A. Keith⁹, Jerzy Klosin¹⁰, Shelley D. Minter¹¹, Robert H. Morris¹², Alexander T. Radosevich¹³, Thomas B. Rauchfuss¹⁴, Neil A. Strotman¹⁵, Aleksandra Vojvodic¹⁶, Thomas R. Ward¹⁷, Jenny Y. Yang¹⁸, Yogesh Surendranath^{13,*}

¹Center for Molecular Electrocatalysis, Pacific Northwest National Laboratory, Richland, WA 99352, USA. ²Department of Chemical Engineering, Columbia University, New York, NY 10027, USA. ³Chemistry Division, Brookhaven National Laboratory, Upton, NY 11973, USA. ⁴Department of Chemistry, Minnesota Supercomputing Institute, and Chemical Theory Center, University of Minnesota, Minneapolis, MN 55455, USA. ⁵Department of Chemistry, Princeton University, Princeton, NJ 08544, USA. ⁶Department of Chemistry and Chemical and Biological Engineering, Northwestern University, Evanston, IL 60208, USA. ⁷Department of Chemistry and Biochemistry, University of Oregon, Eugene, OR 97403, USA. ⁸School of Chemical and Biomolecular Engineering, Georgia Institute of Technology, Atlanta, GA 30332, USA. ⁹Department of Chemical and Petroleum Engineering, University of Pittsburgh, Pittsburgh, PA 15261, USA. ¹⁰Core R&D, Dow Chemical Co., Midland, MI 48674, USA. ¹¹Department of Chemistry, University of Utah, Salt Lake City, UT 84112, USA. ¹²Department of Chemistry, University of Toronto, Toronto, Ontario M5S 3H6, Canada. ¹³Department of Chemistry, Massachusetts Institute of Technology, Cambridge, MA 02139, USA. ¹⁴School of Chemical Sciences, University of Illinois, Urbana, IL 61801, USA. ¹⁵Process Research and Development, Merck & Co. Inc., Rahway, NJ 07065, USA. ¹⁶Department of Chemical and Biomolecular Engineering, University of Pennsylvania, Philadelphia, PA 19104, USA. ¹⁷Department of Chemistry, University of Basel, CH-4058 Basel, Switzerland. ¹⁸Department of Chemistry, University of California, Irvine, CA 92697, USA.

Abstract

Numerous redox transformations that are essential to life are catalyzed by metalloenzymes that feature Earth-abundant metals. In contrast, platinum-group metals have been the cornerstone of many industrial catalytic reactions for decades, providing high activity, thermal stability, and tolerance to chemical poisons. We assert that nature's blueprint provides the fundamental principles for vastly expanding the use of abundant metals in catalysis. We highlight the key physical properties of abundant metals that distinguish them from precious metals, and we look to nature to understand how the inherent attributes of abundant metals can be embraced to produce

*Corresponding author. morris.bullock@pnnl.gov (R.M.B.); jgchen@columbia.edu (J.G.C.); gagliardi@umn.edu (L.G.); yogi@mit.edu (Y.S.).

Competing interests: The authors have no competing interests relevant to this publication.

highly efficient catalysts for reactions crucial to the sustainable production and transformation of fuels and chemicals.

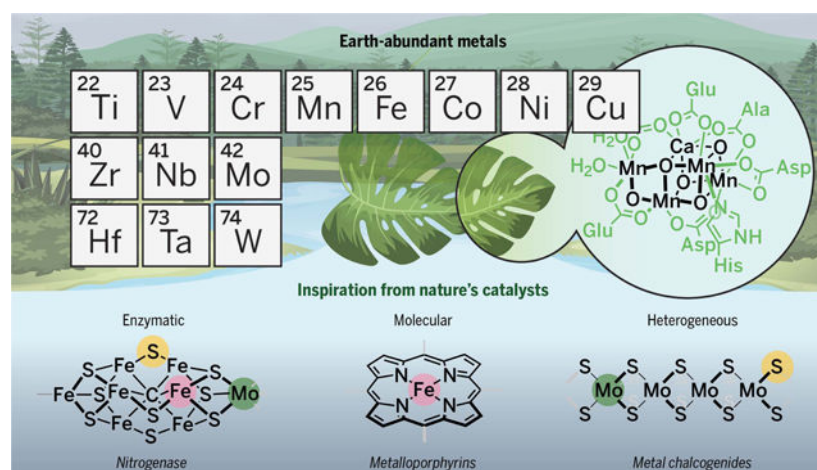
Graphical Abstract

BACKGROUND: Catalysis has had a transformative impact on society, playing a crucial role in the production of modern materials, medicines, fuels, and chemicals. Precious metals have been the cornerstone of many industrial catalytic processes for decades, providing high activity, stability, and tolerance to poisons. In stark contrast, redox catalysis essential to life is carried out by metalloenzymes that feature exclusively Earth-abundant metals (EAMs). The terrestrial abundance of some EAMs is 10^4 times that of precious metals, and thus their increased use would lead to reduced cost and environmental footprint. In addition to these practical considerations, EAMs display distinct reactivity profiles that originate from their characteristic electronic structure, thermochemistry, and kinetics. The behavior of EAMs provides compelling scientific opportunities for catalyst design. We assert that nature's blueprint provides essential principles for vastly expanding the use of EAMs in sustainable catalysis.

ADVANCES: Exquisite tuning of the local environment around EAM active sites is key to enabling their use in catalysis. Such control is achieved in enzymatic catalysis by directed evolution of the amino acid environment, resulting in engineered enzymes with extraordinary catalytic performance. Similarly in molecular catalysis, modifying the steric and electronic properties of ligands can lead to some EAM catalysts with performance superior to that obtained from precious metal catalysts. In addition, for heterogeneous catalysts, the local environment and electronic structure of active sites can be modified by bonding to other metals or main-group elements, facilitating reaction pathways distinct from those involving precious metals. Innovations in the design of EAM catalysts demonstrate their potential to catalyze many of the reactions that traditionally relied on precious metals, although further improvements are needed in activity, selectivity, lifetime, or energy efficiency. The characteristics of EAMs point to an overarching need for improved theories and computational methods that accurately treat their multiconfigurational electronic structure.

OUTLOOK: The remarkable ability of enzymes to catalyze a variety of reactions under mild conditions, using only EAMs, highlights compelling opportunities for the discovery of new catalysis. Although enzymes are versatile platforms for harnessing the properties of EAMs, they are insufficiently robust under the harsh pH, temperature, pressure, and solvent conditions required for some industrial catalytic processes. Thus, systematic strategies are needed for directed evolution to extend the reactivity and persistence of engineered enzymes. For molecular catalysts, the tunability of the ligands provides opportunities for systematically varying the activities of EAMs. Key challenges include enhancing metal-ligand cooperativity, controlling transport to EAM active sites, and mastering the interactions of EAM centers with both metal-based and organic-based redox-active ligands. In heterogeneous catalysis, tuning the lattice environment of EAMs offers new opportunities for catalyst discovery, but for practical applications EAM catalysts should exhibit long-term stability and high active-site density. Thus, advances are needed in the synthesis of materials with tunable phase and nanostructure, as well as insights into how EAM catalysts undergo electronic and structural changes under sustained catalytic turnover. Strategies for controlling EAM reactivity patterns, coupled with advances in synthetic methods and

spectroscopic and computational techniques, are critical for the systematic use of EAMs in sustainable catalysis.



Catalysis by Earth-abundant metals. Nature's blueprint provides the fundamental principles for expanding the use of abundant metals in catalysis by controlling the local environment and electronic structure of metal centers. Examples include nitrogenase-based enzymatic catalysts for N_2 reduction, metalloporphyrin-based molecular catalysts for reduction of oxygen and carbon dioxide, and metal chalcogenides in heterogeneous catalysis for hydrodesulfurization and hydrogen evolution reactions.

Catalysis has had a transformative impact on society, playing a decisive role in the production of modern materials we use daily, medicines to keep us healthy, and fuels for transportation. Most of the key chemical reactions essential to our contemporary lifestyle are catalyzed by transition metals (TMs). The terrestrial abundance of TMs varies over a remarkable range. The first-row (3d) metals of the transition series in the periodic table, as well as the early second-row (4d) and third-row (5d) metals, are relatively abundant, whereas the platinum group metals (PGMs) that constitute the mid- to late portion of the second and third rows have substantially lower crustal abundance (Fig. 1) (1). Here, we highlight frontier opportunities for designing and enabling new catalysts based on Earth-abundant metals (EAMs), with an emphasis on redox reactions crucial to the sustainable production and transformation of fuels and chemicals.

Many redox transformations (2) that are essential to life are catalyzed by EAMs in nature. Because biological organisms must accumulate metals from their surroundings, evolution selected the EAMs exclusively in biological catalysis. Indeed, there are no known native biological catalysts that use a PGM. Consequently, metalloenzymes provide an expansive existence proof that EAMs catalyze complex redox transformations. A tri-Cu active site in the laccase enzyme (3, 4) reduces O_2 to H_2O , a key cathodic reaction in fuel cells. A cluster containing Fe and Mo reduces N_2 to NH_3 in nitrogenase (5). A dinuclear Ni active site catalyzes the CO insertion reaction in acetyl-coenzyme A (CoA) synthase (Fig. 2, top left). Enzymes containing Ni-Fe organometallic complexes carry out the reversible interconversion of H_2 and H^+ in hydrogenase (6) (Fig. 2, middle left). A Mn-Ca cluster catalyzes the oxidation of water to O_2 in photosystem II (7) (Fig. 2, bottom left). The

selective oxidation of methane to methanol occurs at the dinuclear Fe active site in methane monooxygenase (8). Diverse C-H functionalization reactions are catalyzed by Fe-S cluster active sites in radical *S*-adenosylmethionine (SAM) enzymes (9). All of these transformations involve multielectron redox reactions, and most require precise control of the delivery or removal of protons.

In contrast to the extensive use of EAMs in nature, PGMs have historically been the cornerstone of many industrial catalytic reactions for decades, owing to their high catalytic activity, thermal stability, and tolerance to chemical poisons. Pd-catalyzed cross-coupling reactions that form C-C bonds (10) have broad utility and tremendous versatility in pharmaceutical, electronic, and materials applications. A second wave of Pd-catalyzed cross-coupling chemistry has given rise to powerful methods for C-N, C-S, and C-O bond-forming reactions that are widely used (11). Rh-based complexes catalyze the CO insertion reaction, hydroformylation (12) (Fig. 2, top right). Pt is the prototypical catalyst for hydrogen production (13) and oxidation (Fig. 2, middle right). Ir oxide catalyzes the oxidation of water to O₂ (14) in polymer electrolyte membrane (PEM) electrolyzers (Fig. 2, bottom right). C-H oxidation and functionalization reactions have been extensively developed using Pd catalysts (15). Selective hydrogenation reactions required in oil refining and fine chemical synthesis routinely use PGM catalysts. The three-way catalyst in catalytic converters used daily in hundreds of millions of cars requires Pt, Rh, and Pd.

EAM catalysts are attractive for many reasons. The “terawatt challenge” (16) for global energy demand highlights the need to consider the scalability of catalytic materials for sustainable energy conversions. The crustal abundance of EAMs exceeds that of PGMs by a factor of 10⁴ or greater (Fig. 1), leading to costs that differ by similar ratios. Costs are influenced both by abundance and production rate (17). The price of a mole of Rh reached > \$15,000 (USD) as of November 2019, whereas the cost of most EAMs is typically <\$2 per mole (although for many catalytic reactions, the metal cost constitutes only a small fraction of the overall process cost; in the synthesis of pharmaceutical products, the cost of chiral ligands can substantially exceed that of the metal). Prices of PGMs are much more volatile than those of EAMs. Moreover, EAMs generally have lower biological toxicity (18), permitting higher levels of residual EAMs than of PGMs in pharmaceutical products (19). Lastly, the high abundance of EAMs generally leads to a lower environmental footprint associated with their mining and purification relative to PGMs. For example, the production of 1 kg of Rh generates >35,000 kg of CO₂ equivalent, whereas 1 kg of Ni produces only 6.5 kg of CO₂ equivalent (Fig. 1, black bars) (20).

Given the appealing attributes of EAMs noted above, one can ask why PGMs continue to be so prevalent in many industrial catalytic processes. The specific reasons vary according to catalytic application. In general, the requirement for effective integration of a catalyst into an overall process often places stringent constraints on the choice of catalyst. For example, in a fuel cell, the use of fast ion conductivity in Nafion (separating charge transfer between anodes and cathodes) requires an acidic pH, thereby constraining the choice of catalysts to corrosion-resistant PGMs. Likewise, the requirement for high-temperature operations in catalytic converters places stringent requirements on durability, constraining viable replacement of PGMs. In addition, the high capital and energy cost of complex downstream

separations imposes a constraint on the minimum selectivity of catalytic processes, and this consideration may dominate relative to the cost and environmental footprint of the metal catalyst itself. These factors motivate the emphasis on the development of EAM catalysts in tandem with new processes that can circumvent the constraints of current catalytic technologies.

EAM catalysts are currently successfully used in several major industrial processes. The Haber-Bosch reaction, which converts N_2 to ammonia, uses an Fe-based catalyst, despite the higher performance of a Ru-based analog (21). Hydrogenation of CO to methanol is carried out using a Cu/Zn-based catalyst. Hydrogen is produced from water in commercial electrolyzers under basic conditions using Ni/Fe-based catalysts. Olefin oligomerization and polymerizations are carried out worldwide on a tremendous scale using EAMs, dominated by Ti, Zr, and Cr catalysts. Terephthalic acid is produced on a large scale through oxidation of *p*-xylene using Co and Mn catalysts. Some industrial processes are catalyzed by both PGMs and EAMs. For example, hydroformylation is conducted using either Co- or Rh-based catalysts (12), and propane dehydrogenation is carried out on either Pt- or Cr-based catalysts (22). Despite these examples, it remains clear that the scope of EAM catalysis is limited relative to the remarkable diversity of transformations catalyzed by EAMs in nature.

Whereas biology provides an invaluable (although sometimes inscrutable) guide to the broadened implementation of EAMs, industrial catalysis often requires substrates, reactions, and reaction conditions quite different from those in biology; PGM catalysts proliferate in this arena. For example, alkenes, which are derived from petroleum, are processed quite differently by enzymes than by industrial catalysts. With the notable exception of Cu-based ethylene-sensor proteins (23), metal-alkene complexes are unknown in nature, although transfer hydrogenations of C=C bonds are catalyzed by a family of biocatalysts, ene reductases (24). In stark contrast, industrial catalytic transformations of alkenes include polymerization, carbonylation, and metathesis; analogs of these processes are absent from the biocatalysis repertoire. Instead, alkenes are often processed in natural systems by attacking weakened allylic C-H bonds using iron-oxo-based radicals (25).

Considering the diversity of catalysis performed by biological systems, a central challenge revolves around coaxing biological macromolecules into displaying entirely abiotic reactivity/ selectivity/stability characteristics that have traditionally been the domain of PGM-based catalysts. A daunting challenge in designing bio-inspired catalysts is to identify and replicate only the parts of the metalloenzyme structure (first, second, or outer coordination sphere) that are thought to be required for catalytic activity, recognizing that while biological reaction networks must maintain life, their catalytic functionality may be accessible from synthetically simpler structures. Replicating the active site is necessary but not sufficient for achieving catalysis comparable to that found in enzymes, as dynamics and conformational changes often exert a large influence on enzymatic catalysis (26).

The considerations discussed above have fueled burgeoning interest in developing new EAM-based catalysts. We assert that this endeavor is best advanced by establishing the fundamental science of EAMs that embraces their particular physical properties and resultant catalytic activities. Herein, we put forward the premise that nature's blueprint

provides the fundamental principles for vastly expanding the use of EAMs in catalysis. We highlight the key physical properties of EAMs that distinguish their reactivity from those of PGMs, and then seek to understand how the inherent attributes of EAMs can be embraced, leading to highly efficient catalysis. Building on that foundation, we identify compelling opportunities for the increased use of EAMs in enzymatic, molecular, and heterogeneous catalysis.

The origins of divergent reactivity between EAMs and PGMs

Electronic structure

The distinctive reactivity profiles of EAMs relative to PGMs originate from fundamental differences arising from periodic trends of the elements (27). In particular, 3d orbitals extend to a lesser extent beyond the 3s and 3p orbitals (28), leading to attenuated orbital overlap with bonding partners, relative to the corresponding 4d and 5d counterparts. This overlap deficit has a considerable impact on the electronic structure of 3d metal-based catalysts. For molecular TM complexes, the overlap deficit leads to more ionic character in metal-ligand bonds and a small frontier d-orbital splitting (Fig. 3, top), stabilizing high-spin electronic configurations. High spin configurations are extremely rare (29, 30) among 4d and 5d TM complexes owing to their much higher frontier orbital splitting energies (Fig. 3, top). Similar phenomena are observed for extended solids: Attenuated orbital overlap between 3d metal atoms leads to a diminished spread in the d-band energies and a corresponding increase in the d-band center of 3d metals relative to the 4d and 5d counterparts (Fig. 3, top). The prevalence of high-spin electronic configurations among 3d TMs has important implications for reactivity (31). Homogeneous PGM catalysts typically cycle through two-electron processes, including familiar examples of oxidative addition/reductive elimination of $\text{Rh}^{\text{I}}/\text{Rh}^{\text{III}}$ and $\text{Pd}^{\text{0}}/\text{Pd}^{\text{II}}$. In contrast, 3d TM complexes more readily engage in single-electron bond activation reactions, including M-X bond homolysis. Additionally, the availability of multiple spin states among EAMs can lead to multistate acceleration of certain reactions.

Thermochemistry

The differences in the electronic structures of EAMs and PGMs are manifested in the thermochemistry of interactions of metals with ligands, reactants, products, and intermediates. The classical Sabatier principle states that an optimal catalyst should bind intermediates neither too strongly nor too weakly, essentially a “Goldilocks” effect (21). In general, bonding to 3d TMs in molecular complexes is weaker relative to 4d/5d TM centers with the same ancillary ligand environment. For example, the bond dissociation energies of the M-H bond in $\text{MH}(\eta^5\text{-C}_5\text{H}_5)(\text{CO})_2$ are 68 kcal/mol (32), 77 kcal/mol (32), and 82 kcal/mol (33) for Fe, Ru, and Os, respectively; for $\text{MH}(\text{CO})_5$, the values are 68 kcal/mol and 75 kcal/mol for Mn and Re, respectively (34). Additionally, the greater extension of the d-orbitals of the second and third TMs also provides for stronger back-bonding interactions with π -accepting ligands, such as CO and olefins, increasing their binding strength. Intermediates bearing such ligands are critical in a number of industrially important processes such as hydroformylation.

The differences in metal bonding thermochemistry are also mirrored in changes in the reduction potentials of metal ions. PGMs are commonly referred to as noble because of their resistance to oxidation, a reflection of their much higher reduction potentials and of the lower O-atom affinities of 4d and 5d metals (Fig. 3, middle, black) relative to 3d TMs (Fig. 3, middle, blue). For example, whereas the Pt^{II/0} and Pd^{II/0} reduction potentials are 1.18 and 0.951 V, respectively, versus the standard hydrogen electrode (SHE), the corresponding Ni^{II/0} reduction potential, -0.26 V, is lower by more than 1 V. Likewise, Pt (111) and Pd (111) surfaces have an O-atom affinity of ~0.5 eV (12 kcal/mol), whereas Ni (111) surfaces have an O-atom affinity of ~4 eV (92 kcal/mol) (Fig. 3). Because these baseline reduction potentials correspond to interconversion of the metallic solid and aquated metal ions, they are influenced by the coordination, electrostatic, and hydrogen-bonding environment of the metal center (35). Because of these effects, the active-site EAMs in metalloenzymes span a wide range of potentials (2) that differ substantially from their baseline values. Similar potential ranges can be accessible through changes in the coordination environment of synthetic coordination compounds (36).

The differences in reduction potential between EAMs and PGMs are of central importance in electrocatalysis, where electron flow drives the conversion of reactants to products. For example, the very positive potential for oxidizing Pt allows it to avoid corrosion at the oxidizing potentials of the O₂/H₂O couple in fuel cells, making it the only currently viable corrosion-resistant cathode catalyst for PEM fuel cells. To achieve similar feats, enzymes such as multi-copper oxidases, laccases (3, 4), and cytochrome c oxidase (37) use an ensemble of metal centers organized within the protein environment that markedly alters their redox properties and oxophilicities.

Kinetics

Owing to their weaker metal-ligand bonds, complexes of the 3d metals are much more labile than their 4d and 5d counterparts (Fig. 3, bottom). The rate accelerations can be extraordinary: Exchange of a water ligand on a high-spin Fe(III) center is faster than on Ru(III) by a factor of 10⁸ (38). We emphasize that lability is a kinetic phenomenon; many labile complexes are thermodynamically stable. Although typically viewed as an impediment to understanding catalytic reactivity, the higher lability of EAMs can, in principle, be beneficial for catalysis. Turnover frequencies are often strongly influenced by the rates of association and dissociation of reactants and products, a manifestation of the Sabatier principle (21). Thus, the inherently higher rate of ligand exchange on the 3d TMs offers the opportunity for rapid catalysis. Two key properties sought are kinetic stability of the metal-supporting ligand ensemble and labile coordination sites with appropriate affinities for substrates. The challenge arises from the fact that lability of EAMs can also lead to the rapid exchange of supporting ligands that tune the local electronic structure and reaction environment of the metal center. To circumvent problems with lability in molecular complexes, polydentate ligands are often used to strongly sequester the metal ion while preserving one or more coordination sites for catalysis. Consequently, tridentate or tetradentate ligands are ubiquitous in catalysis by synthetic 3d TMs relative to PGMs, so as to overcome the inherent differences in lability relative to PGMs. The premier examples of

multidentate ligands in biocatalysis are porphyrins, where four metal-nitrogen bonds confer substantial kinetic inertness.

In extended solids, the kinetics of substitution at EAMs also play a central role in the longevity of catalysts. The weaker M-lattice bonding in mid- to late 3d metal and metal oxide materials contributes to their high propensity to sinter, restructure, become amorphous, and corrode under catalytic conditions, relative to 4d and 5d analogs. A richer understanding of how to control metal lability in extended solids is essential for creating robust EAM catalysts, particularly for harsh reaction environments.

Computational insights

Much of our physical understanding of EAMs has been enhanced through consistent benchmarking between experiment and theory. A comprehensive understanding of EAM reactivity will require a refined understanding of electronic structure, thermochemistry, and kinetics. Yet current theoretical tools that are effective at modeling multiconfigurational electronic structure commonplace among EAMs are often ineffective for predicting thermochemical and kinetic properties (39). This impasse results from the enormous computational expense required to calculate the properties of EAMs that reside in shallow potential energy wells with a diversity of available spin configurations.

The widely used density functional theory (DFT) has strengths and weaknesses, and both are highlighted in modeling catalysis by EAMs. In some cases, trends can be identified readily using simple basis sets and commonly used functionals. Often complementing experimental results, theoretical studies can identify rate-determining steps, assign vibrational bands, and determine redox potentials. Useful thermochemical predictions of energies can often be obtained, even if specific spin states may not be easily determined reliably. Spin transitions and d-orbital splitting of EAMs are difficult to treat because states that are very similar in energy occur frequently with EAMs.

Machine learning (ML)-based methods have generated enormous recent interest in the computational analysis of catalysis (40). In a typical application of ML, large datasets (often resulting from thousands of DFT calculations) are used for statistical regression analyses with ML methods to identify the most accurately parametrized model for the dataset. A well-trained ML model should successfully interpolate within the chemical/materials space of the training data and be useful for screening molecular/ material properties for hypothetical homogeneous (41, 42) and/or heterogeneous (43, 44) catalyst active sites across larger regions of chemical and materials space than are accessible with DFT calculations alone. Complementary to ML approaches, theoretical schemes such as alchemical perturbation DFT allow rapid screening of adsorbate binding energies (45) with minimal precalculated reference data and low computational cost.

Emerging opportunities for catalytic reactivity of EAMs

Recent progress in the design of EAM catalysts demonstrates their potential in many reactions that traditionally use PGMs, although they often fall short of the performance of PGM catalysts on one or more benchmarks (46): activity, selectivity, lifetime, or energy

efficiency. Yet EAM-based enzymes have evolved in nature to facilitate an impressively diverse array of reactions. We assert that nature's blueprint provides invaluable guidance for frontier areas of exploration in EAM catalysis that takes advantage of the inherent electronic structure, thermodynamic, and kinetic characteristics of EAMs. We discuss below how to use biologically inspired approaches to design EAM catalysts with enhanced performance in the context of enzymatic, molecular, and heterogeneous reactivity.

Enzymatic catalysis

Biological catalysts with TM active sites feature exclusively EAMs; a central challenge revolves around modifying enzymes to display abiotic functions (Fig. 4). Many metalloenzymes display promiscuous activities (47), a feature that provides a diversity of reactivity for the discovery of abiotic enzymatic catalysis. There has been increasing recognition that biological cofactors featuring EAMs are active, albeit at a low level, for a wide array of abiotic transformations that are commonly carried out by synthetic PGM-based catalysts. For example, carbene insertion reactions, which enable the rapid elaboration of simple organic feedstocks into fine and pharmaceutical chemicals, are catalyzed efficiently by synthetic Rh-based catalysts (48). Remarkably, many native hemoproteins also display low-level activity for these same reactions, and directed evolution of these enzymes has led to a family of biocatalysts (49) with excellent activity and selectivity for carbene insertion into C-H, N-H, and Si-H bonds. The activity and selectivity of these evolved metalloproteins now rival and even exceed those of Rh-based catalysts. One recent study (50) showed that hemoproteins can be repurposed to catalyze carbon-carbon bond formation by insertion of a carbene, rather than oxygen, into a C-H bond—a reaction traditionally dominated by PGMs (51). Implementing the blueprint from nature requires precise control of the local environment by modifying the active site to bind an abiotic reactant, such as a carbene, while minimizing the binding of the native substrate (i.e., O₂) with exquisite selectivity (52). The fundamental workflow of protein engineering—identifying promiscuous reactivity for abiotic substrates, then using protein-engineering tools to maximize performance—serves as a valuable blueprint for further advances in catalysis of abiotic reactions. Continued progress to expand the palette of enzymatic catalysis will benefit from the development of new methods for identifying enzyme candidates and strategies for accelerating directed evolution and selection of high-performance mutant enzymes.

The macromolecular scaffolds that house EAM active sites in enzymes are critical to their function but invariably afford high-molecular weight catalysts. For commodity-scale catalysis, the density of active sites is a critical determinant of space-time yield, imposing constraints on overall performance. In some cases, subunits of enzymes can be discarded without greatly lowering catalytic efficiency; this suggests that there is ample opportunity for enhancing active-site density without necessarily decreasing the turnover frequency or selectivity of each site. In other cases, mutation of a single amino acid remote from the active site can appreciably alter catalytic performance (53). Reliable methods for discriminating the portions of the enzyme scaffold that are essential for catalysis from those that are not necessary will facilitate the wider use of enzymatic EAM catalysis for large-scale industrial processes.

Many abiotic reactions of critical importance are ideally performed under conditions (temperature, pressure, pH) that are far removed from the mild conditions of biology. For example, catalysts in fuel cells and electrolyzers often operate at the extremes of pH to facilitate ion conduction, and many heterogeneous catalysts operate at elevated temperatures to enhance the reaction rate and facilitate heat integration. Biological systems offer opportunities for adapting enzyme catalysis to extreme reaction conditions. In particular, thermophilic archaea sustain life processes at temperatures exceeding 100°C and at extremes of pH (54). It has long been recognized that some enzymes display enhanced catalytic activity in organic solvents (55), yet there remains limited fundamental understanding of the characteristics of enzymes that engender persistent activity under these conditions. Additionally, whereas abiotic reactivity modes can be screened using abiotic reagents, screening for enzymatic performance under abiotic reaction conditions is more difficult because the biological replication machinery operates within a narrow domain of conditions. Strategies for driving directed evolution within extremophile hosts, and a deeper understanding of the factors that contribute to protein stability, provide plentiful opportunities for extending the rich EAM catalytic reactivity of enzymes toward the harsher conditions often required for thermal and electrochemical catalysis.

Molecular catalysis

The modern molecular synthetic toolkit affords virtually unlimited scope for tailoring the primary, secondary, and outer coordination spheres around a molecular EAM active site. Several areas of exploration leverage this synthetic capability to embrace the distinctive physical properties of EAMs (Fig. 5).

EAM active sites in nature are subject to exquisite tuning by the arrangement of proximal amino acid residues and cofactors, as well as by the enzyme channels that gate the transport of reactants and products in and out. Similarly, achieving precise control over the local environment and transport in synthetic molecular EAM catalysts is critical for realizing their full potential. The ability to synthesize increasingly sophisticated ligands provides control of steric and electronic attributes, as demonstrated by remarkable progress in asymmetric hydrogenations, which are used extensively to achieve the enantioselectivity required in the preparation of pharmaceuticals and agrochemicals. This field has been dominated by Rh- and Ru-based catalysts with chiral diphosphines (56), but recent examples show that EAM catalysts can offer outstanding selectivity. For example, an Fe complex catalyzes the asymmetric transfer hydrogenation of ketones with performance superior to that of Ru catalysts (57), and a Co complex catalyzes the asymmetric hydrogenation of the C=C bond of enamides (58).

In addition to modifications of the ligands bound directly to the metal (primary coordination sphere), the environment of molecular catalysts can be tuned by positioning secondary coordination sphere substituents, such as Lewis acids (59), positively charged groups (60–62), hydrogen bond donors (63), and pendant amines functioning as proton relays (64–68) (Fig. 5A) proximal to the EAM center. These strategies have enhanced the rates of molecular EAM catalysis of electrochemical H₂ evolution (64–66), H₂ oxidation (65, 66, 68), CO₂ reduction (60), and O₂ reduction (69). Because the redox reactivity involves coupling of

electron flow and bond rearrangement, the secondary coordination sphere substituents must be precisely positioned to foster optimal cooperativity. For example, the rates of proton-coupled electron transfer (70, 71) can be sensitive to sub-angstrom-level changes in the distance between proton donor and acceptor (72). Cooperativity between the primary and secondary coordination spheres in enzymes is achieved through the dynamic flexibility of the protein scaffold (26), a property that is difficult to recreate systematically in synthetic EAM catalysts. Strong electric fields can influence enzyme catalysis (73) by manipulating the energies of intermediates or transition states, thereby changing the rates and selectivity. Computations offer the opportunity to prescreen the impact of positioning of the secondary coordination sphere moieties; such studies could motivate synthetic efforts toward optimized secondary coordination sphere control in EAM catalysis.

Controlling transport to EAM active sites is difficult to achieve with freely diffusing small molecules, but improved transport environments can be created by anchoring molecular EAM active sites on the surfaces of, or within the pores of, extended solid host materials including, for example, graphitic carbon, microporous silica, and metal-organic frameworks (MOFs) (74). Solid-supported site-isolated EAMs have been used to catalyze a wide array of reactions; they benefit from structural constraints that prevent inhibitory bimolecular reactivity between metal centers while facilitating catalyst separation and recycling. For these molecular materials, the extended lattice can serve as scaffolding to incorporate secondary coordination sphere elements proximate to the embedded active site, and the pore structure and dimensions can be used to gate the transport of reactants and products to and from the active site. MOFs with EAM active sites have been deployed to carry out, for example, photocatalytic CO₂ reduction (75), ethylene hydrogenation (76), oxidation of alcohols (77), olefin cyclopropanation (78), arene C-H borylation (79), tandem oxidation and functionalization of styrene (80), and selective oxidation of methane to methanol (81). Enzymes often feature disparate channels that transport each reactant and product molecule in different directions, with the EAM active sites precisely positioned at the junction of these conduits. Similar precision has been difficult to achieve in synthetic systems, and efforts toward constructing molecular materials with active sites at the intersection of multiple transport conduits could substantially advance selectivity in EAM catalysis.

Because of their low field strengths, EAM complexes have a propensity to undergo single-electron transfer pathways (82). The control levers noted above are particularly important for embracing and controlling radical reactivity. Because of their smaller d-orbital splitting and weaker spin-pairing energy, EAMs tend to react in enzymes through radical intermediates. Controlled radical reactions are central to biological detoxification by heme centers in cytochrome P450 enzymes, the synthesis of DNA precursors mediated by ribonucleotide reductase, and many other critical transformations mediated by cobalamins and radical SAM enzymes (9). By controlling the reactivity of Co(III) carbon-centered radicals generated from Co(II) porphyrin complexes, eight-membered rings have been produced from ring-closing reactions; this strategy provides attractive synthetic methods for reactions that traditionally required precious metal catalysts (83). Cooperative catalysis using EAM complexes of two metals, Ti and Cr, has provided a highly selective route to anti-Markovnikov alcohols through ring-opening of epoxides (84). This hydrogenation of

epoxides is unusual because at different steps of the mechanism, a chromium complex transfers an electron, a hydrogen atom, and a proton.

Aerobic oxidation of primary alcohols to aldehydes and H_2O_2 is catalyzed in natural systems by galactose oxidase, a copper-containing enzyme. A bio-inspired synthetic binuclear copper complex exhibiting metal-ligand cooperative reactivity catalyzes the oxidation of primary alcohols using O_2 from air (85). Similar to the accepted mechanism for galactose oxidase, the rate-determining step of the synthetic system is proposed to involve hydrogen atom transfer from a C-H bond of the alcohol to the oxygen-centered radical bound to Cu.

Many of the EAM active sites that occur naturally, particularly those carrying out multielectron redox transformations, feature multiple metal centers linked to each other in cluster active sites or metal centers coupled to redox-active cofactor ligands. The presence of these additional metals and redox-active ligands expands the number of available redox states accessible over a range of potentials. This increased density of electron states serves to buffer redox changes at the metal center that binds and activates the reactant, thereby lowering the energy barrier to multielectron transformations. Harnessing the full power of EAMs in synthetic catalysts will require mastering the interactions of EAM centers with both metal-based and organic-based redox active ligands.

EAMs with redox-active ligands (86–88) catalyze a wide variety of reactions, including cleavage of C-C bonds (89), cycloadditions (90), oxidation of alcohols (91), and aminations (92). Further systematic deployment of redox-active ligands in EAM catalysis will benefit from general design rules for independently tuning metal-based and ligand-based redox levels to control the thermochemistry of elementary reaction steps. These ligands also play a key role in electrocatalysis at molecular active sites by providing a reservoir for accumulating redox equivalents that are cumulatively discharged to promote multielectron reactions including, for example, CO_2 reduction (93) and O_2 reduction (94). An improved understanding of how to design systems with enhanced metal/ligand redox cooperativity would facilitate the design of more efficient (electro)catalysts.

Coupling between the metal binding site and one or more metals can also increase the density of electronic states available for a multielectron transformation. Bimetallic and multimetallic EAM catalysts have been used for CO_2 reduction (Fig. 5B) (95, 96), cycloadditions (Fig. 5D) (90), dehydrogenation of formic acid (97), and reduction of NO_2 (67) or O_2 (98). Further systematic development of multimetallic systems in EAM catalysis will benefit from a better understanding of how to stabilize the cluster against irreversible fragmentation while retaining the capacity to rapidly break and regenerate M-M or M-E-M (E = S, O) bonds during a catalytic cycle.

Understanding molecular EAM catalysts in systems with an increased density of states requires new spectroscopic tools and computational methods (99). Whereas current computational methods effectively model weakly correlated closed-shell singlets, new methods are needed for accurately modeling open-shell species, and deconvolution of spin-state populations is required to accurately model the multiconfigurational electronic

structure of metal clusters and metal complexes involving redox-active ligands (100). Open-shell systems are often paramagnetic and intractable to characterize by routine nuclear magnetic resonance methods; emerging improved spectroscopic tools for characterizing paramagnetic species are advancing mechanistic understanding of these systems (101–103).

Heterogeneous catalysis

Heterogeneous catalysis occurs on the surfaces of extended solids. Although these extended solids may bear little direct structural resemblance to active sites in nature, the principles that define EAM catalysis in enzymes provide valuable leads toward their greater utility in heterogeneous catalysis.

Similar to the catalytic cooperativity in nature, enhanced catalytic performance can emerge from extended solids that incorporate multiple EAMs acting cooperatively. For example, by combining the different binding strengths of Ti and Cu toward hydrogen, alloying Ti and Cu leads to hydrogen evolution reactivity similar to that of PGMs (104). Analogously, mixed oxyhydroxides containing Fe, Co, and W catalyze oxygen evolution in an alkaline environment (105); the cooperative interactions of even trace amounts of Fe can profoundly promote oxygen evolution activity on NiOOH (Fig. 6B) (106). Considering the inherent lability of EAMs, improved characterization tools are needed to track the time dependence of surface restructuring in multimetallic EAM catalysts. Additionally, multimetallic EAM oxide-based catalytic materials are challenging to model with conventional computational methods (107); detailed mechanistic understanding of these systems would benefit from new computational tools that effectively model compositional heterogeneity and extend multiconfigurational methods to periodic solids. Given the enormous compositional diversity available in multimetallic solids, machine learning tools offer the potential to explore multidimensional reaction landscapes rapidly.

Historically, EAM heterogeneous catalysis focused predominantly on the reactivity of metal or metal oxide phases, the two endpoint thermodynamic sinks under reducing or oxidizing conditions, respectively. In contrast, many EAM active sites in nature are hosted within highly evolved combinations of sulfur, nitrogen, and carbon in the primary coordination environments, suggesting an appealing opportunity to exploit new types of heterogeneous catalysts. Relative to the O atoms in oxide host lattices, the greater orbital extension and/or energetic match of the p-orbitals in C, N, P, and S with the d-orbitals of EAMs leads to substantial changes in the band structures of chalcogenides (108, 109), pnictides (110–112), and carbides (110, 113), potentially endowing these EAM catalysts with enhanced activity relative to the corresponding metal or oxide phases. For example, metal sulfide and phosphide materials have emerged as potent catalysts for electrochemical hydrogen evolution (109), and EAM carbides have been shown to be highly selective for hydrodeoxygenation of biomass-derived molecules (114). Considering the vast phase space available among chalcogenides, pnictides, and carbides, there is ample opportunity to discover new EAM catalysts that take advantage of environments akin to those found in nature. Progress toward these goals will require advances in the synthesis of materials with tunable phase and nanostructure at sufficient scales for catalytic applications. In addition, because these materials are typically metastable relative to their corresponding metal or

oxide phases, fundamental insights are needed to understand how the surfaces of these materials undergo reconstruction under sustained catalytic turnover (115). Surface-sensitive operando spectroscopic characterization (116) revealing the chemical stability of these materials is critical for the design of optimal catalysis.

EAM active sites can also be hosted within graphitic carbon host lattices. For many decades, it has been recognized that the high-temperature pyrolysis of nitrogen and carbon precursors bound to EAMs such as Fe and Co can lead to the generation of relatively high-performance electrocatalysts for the oxygen reduction reaction in fuel cells (117, 118). These materials, often referred to as M-N-C catalysts, are postulated to contain metal nanoparticles and mononuclear metal sites embedded in the graphitic framework, with varying ratios depending on the synthetic conditions (119). Fe-N-C materials are leading EAM candidates to replace Pt in fuel cells, and this class of materials presents an opportunity to create emergent reactivity from EAMs through strong interaction between the EAM orbitals and the electronic states of graphitic carbons. Despite decades of work in this area, the local structure of the active sites remains poorly understood, and the synthetic toolkit for tuning the population of active sites remains limited. Thus, continued progress in this area will hinge on new strategies for better understanding and controlling the inherent distribution of active-site structures present in these materials.

The microenvironment around the active site in natural systems is precisely controlled by preorganizing reactants, imposing a local electric field, and controlling transport to and from active sites. The dynamic nature of EAMs affords opportunities to implement these concepts within heterogeneous catalysts. Many strategies have been used for imposing a particular microenvironment at the catalyst surface: For catalysis at solid-liquid interfaces, the composition of the solvent or electrolyte can be varied; the catalyst can be designed with appropriate meso/microstructure to create diffusional gradients at the surface; and the catalyst surface can be chemically modified (120). Electrolyte choice, catalyst mesostructuring, and chemical modification have all been applied to tune the selectivity of Cu-based CO₂/CO reduction catalysts (121). The solution environment can also be used to favor mechanisms for dynamic self-repair of catalysts; for example, Co ions in solution promote dynamic stability and self-repair of Co-based oxygen evolution catalysts that would otherwise undergo corrosion (122). Additionally, thin gas-permeable layers of ionic liquids (123) and/or molecular promoters could create specific microenvironments that contain substrate-binding units proximate to active sites. This strategy enhances the stability of EAMs prone to irreversible reconstruction/oxidation, and may also foster improved selectivity. Despite the enormous synthetic opportunities in this area, mechanistic insights into how local microenvironments tune heterogeneous catalysis are rare. Although there are many tools for operando characterization of catalysts, these tools often only shed light on the primary coordination environments of EAM active sites. Thus, improved tools are needed for characterizing longer-range interactions in the secondary and outer coordination spheres that define the microenvironment of the catalyst. Notwithstanding these formidable challenges, the tantalizing prospect of creating enzyme-like three-dimensional active sites on surfaces has enormous appeal for emerging EAM catalysis.

Outlook

Recent years have seen tremendous growth in the development and application of EAM catalysts; however, the fundamental understanding of reactivity patterns of these metals has lagged behind that of PGMs. This disparity in both understanding and use of EAMs is attributed to the broader landscape of reactivity available to EAMs and the smaller historical investment devoted to the study of them. The gaps in fundamental scientific knowledge highlighted here are intended as a “call to action” to identify and overcome scientific barriers to EAM catalysis, based on compelling opportunities that embrace and exploit the characteristic reactivity of EAMs. Examples of recent discoveries of EAM catalysts that rival, or even exceed, the performance of PGM catalysts document the value of identifying design principles for new classes of catalysts. In addition to catalytic activity, EAM catalysts should possess long-term stability and high active-site density for practical applications. The quest to develop efficient, sustainable catalysts based on EAMs benefits from cohesive efforts in synthesis, operando characterization, mechanistic inquiry, materials design, and theoretical modeling. Spurred by recent advances, the collective efforts of the catalysis community can bring the full potential of EAM catalysts to realization.

ACKNOWLEDGMENTS

We gratefully acknowledge the Division of Chemical Sciences, Geosciences and Biosciences of the U.S. Department of Energy, Office of Science, Office of Basic Energy Sciences. This article evolved from presentations and discussions at the workshop “Earth-Abundant Metal Catalysis” held in April 2019 in Gaithersburg, Maryland.

REFERENCES AND NOTES

1. CRC Handbook of Chemistry and Physics, 97th Edition (CRC Press, 2016).
2. Liu J et al., Metalloproteins containing cytochrome, iron-sulfur, or copper redox centers. *Chem. Rev* 114, 4366–4469 (2014). doi: 10.1021/cr400479b; [PubMed: 24758379]
3. Thorseth MA, Tornow CE, Tse ECM, Gewirth AA, Cu complexes that catalyze the oxygen reduction reaction. *Coord. Chem. Rev* 257, 130–139 (2013). doi: 10.1016/j.ccr.2012.03.033
4. Solomon EI et al., Copper active sites in biology. *Chem. Rev* 114, 3659–3853 (2014). doi: 10.1021/cr400327t; [PubMed: 24588098]
5. Seefeldt LC et al., Energy Transduction in Nitrogenase. *Acc. Chem. Res* 51, 2179–2186 (2018). doi: 10.1021/acs.accounts.8b00112; [PubMed: 30095253]
6. Lubitz W, Ogata H, Rüdiger O, Reijerse E, Hydrogenases. *Chem. Rev* 114, 4081–4148 (2014). doi: 10.1021/cr4005814; [PubMed: 24655035]
7. McEvoy JP, Brudvig GW, Water-splitting chemistry of photosystem II. *Chem. Rev* 106, 4455–4483 (2006).doi: 10.1021/cr0204294; [PubMed: 17091926]
8. Wang VCC et al., Alkane Oxidation: Methane Monooxygenases, Related Enzymes, and Their Biomimetics. *Chem. Rev* 117, 8574–8621 (2017). doi: 10.1021/acs.chemrev.6b00624; [PubMed: 28206744]
9. Broderick JB, Duffus BR, Duschene KS, Shepard EM, Radical *S*-adenosylmethionine enzymes. *Chem. Rev* 114, 4229–4317 (2014). doi: 10.1021/cr4004709; [PubMed: 24476342]
10. Johansson Seechurn CCC, Kitching MO, Colacot TJ, Snieckus V, Palladium-catalyzed cross-coupling: A historical contextual perspective to the 2010 Nobel Prize. *Angew. Chem. Int. Ed* 51, 5062–5085 (2012). doi: 10.1002/anie.201107017;
11. Dorel R, Grugel CP, Haydl AM, The Buchwald-Hartwig Amination After 25 Years. *Angew. Chem. Int. Ed* 58, 17118–17129 (2019). doi: 10.1002/anie.201904795;
12. Franke R, Selent D, Börner A, Applied hydroformylation. *Chem. Rev* 112, 5675–5732 (2012). doi: 10.1021/cr3001803; [PubMed: 22937803]

13. Nørskov JK et al., Trends in the Exchange Current for Hydrogen Evolution. *J. Electrochem. Soc* 152, J23–J26 (2005). doi: 10.1149/1.1856988
14. McCrory CCL, Jung S, Peters JC, Jaramillo TF, Benchmarking heterogeneous electrocatalysts for the oxygen evolution reaction. *J. Am. Chem. Soc* 135, 16977–16987 (2013). doi: 10.1021/ja407115p; [PubMed: 24171402]
15. Hartwig JF, Evolution of C-H Bond Functionalization from Methane to Methodology. *J. Am. Chem. Soc* 138, 2–24 (2016). doi: 10.1021/jacs.5b08707; [PubMed: 26566092]
16. Smalley RE, Future Global Energy Prosperity: The Terawatt Challenge. *MRS Bull.* 30, 412–417 (2005). doi: 10.1557/mrs2005.124
17. Vesborg PCK, Jaramillo TF, Addressing the terawatt challenge: Scalability in the supply of chemical elements for renewable energy. *RSC Adv.* 2, 7933–7947 (2012).doi: 10.1039/c2ra20839c
18. Egorova KS, Ananikov VP, Toxicity of Metal Compounds: Knowledge and Myths. *Organometallics* 36, 4071–4090 (2017). doi: 10.1021/acs.organomet.7b00605
19. Hayler JD, Leahy DK, Simmons EM, A Pharmaceutical Industry Perspective on Sustainable Metal Catalysis. *Organometallics* 38, 36–46 (2019). doi: 10.1021/acs.organomet.8b00566
20. Nuss P, Eckelman MJ, Life cycle assessment of metals: A scientific synthesis. *PLOS ONE* 9, e101298 (2014).doi: 10.1371/journal.pone.0101298; [PubMed: 24999810]
21. Medford AJ et al., From the Sabatier principle to a predictive theory of transition-metal heterogeneous catalysis. *J. Catal* 328, 36–42 (2015). doi: 10.1016/j.jcat.2014.12.033
22. Sattler JJHB, Ruiz-Martinez J, Santillan-Jimenez E, Weckhuysen BM, Catalytic dehydrogenation of light alkanes on metals and metal oxides. *Chem. Rev* 114, 10613–10653 (2014). doi: 10.1021/cr5002436; [PubMed: 25163050]
23. Light KM, Wisniewski JA, Vinyard WA, Kieber-Emmons MT, Perception of the plant hormone ethylene: Known-knowns and known-unknowns. *J. Biol. Inorg. Chem* 21, 715–728 (2016). doi: 10.1007/s00775-016-1378-3; [PubMed: 27456611]
24. Toogood HS, Scrutton NS, Discovery, Characterisation, Engineering and Applications of Ene Reductases for Industrial Biocatalysis. *ACS Catal.* 8, 3532–3549 (2019). doi: 10.1021/acscatal.8b00624; [PubMed: 31157123]
25. Costas M, Mehn MP, Jensen MP, Que L Jr., Dioxygen activation at mononuclear nonheme iron active sites: Enzymes, models, and intermediates. *Chem. Rev* 104, 939–986 (2004). doi: 10.1021/cr020628n; [PubMed: 14871146]
26. Hammes GG, Benkovic SJ, Hammes-Schiffer S, Flexibility, diversity, and cooperativity: Pillars of enzyme catalysis. *Biochemistry* 50, 10422–10430 (2011). doi: 10.1021/bi201486f; [PubMed: 22029278]
27. McCusker JK, Electronic structure in the transition metal block and its implications for light harvesting. *Science* 363, 484–488 (2019). doi: 10.1126/science.aav9104; [PubMed: 30705184]
28. Pyykko P, Relativistic Effects in Structural Chemistry. *Chem. Rev* 88, 563–594 (1988). doi: 10.1021/cr00085a006
29. Watson LA, Ozerov OV, Pink M, Caulton KG, Four-coordinate, planar RuII. A triplet state as a response to a 14-valence electron configuration. *J. Am. Chem. Soc* 125, 8426–8427 (2003). doi: 10.1021/ja035166p; [PubMed: 12848535]
30. Kinauer M et al., An iridium(III/IV/V) redox series featuring a terminal imido complex with triplet ground state. *Chem. Sci* 9, 4325–4332 (2018). doi: 10.1039/C8SC01113C; [PubMed: 29780564]
31. Swart M, Costas M, Eds., Spin States in Biochemistry and Inorganic Chemistry: Influence on Structure and Reactivity (Wiley, 2016).
32. Estes DP, Vannucci AK, Hall AR, Lichtenberger DL, Norton JR, Thermodynamics of the Metal-Hydrogen Bonds in (η^5 -C₅H₅)M(CO)₂H (M = Fe, Ru, Os). *Organometallics* 30, 3444–3447 (2011). doi: 10.1021/om2001519
33. Zhang J, Grills DC, Huang K-W, Fujita E, Bullock RM, Carbon-to-metal hydrogen atom transfer: Direct observation using time-resolved infrared spectroscopy. *J. Am. Chem. Soc* 127, 15684–15685 (2005). doi: 10.1021/ja0555724; [PubMed: 16277493]
34. Parker VD, Handoo KL, Roness F, Tilset M, Electrode Potentials and Thermodynamics of Isodesmic Reactions. *J. Am. Chem. Soc* 113, 7493–7498 (1991). doi: 10.1021/ja00020a007

35. Marshall NM et al., Rationally tuning the reduction potential of a single cupredoxin beyond the natural range. *Nature* 462, 113–116 (2009). doi: 10.1038/nature08551; [PubMed: 19890331]
36. Lever ABP, Electrochemical Parametrization of Metal Complex Redox Potentials, Using the Ruthenium(III)/ruthenium(II) Couple to Generate a Ligand Electrochemical Series. *Inorg. Chem* 29, 1271–1285 (1990). doi: 10.1021/ic00331a030
37. Wikström M, Krab K, Sharma V, Oxygen Activation and Energy Conservation by Cytochrome *c* Oxidase. *Chem. Rev* 118, 2469–2490 (2018). doi: 10.1021/acs.chemrev.7b00664; [PubMed: 29350917]
38. Helm L, Merbach AE, Inorganic and bioinorganic solvent exchange mechanisms. *Chem. Rev* 105, 1923–1959 (2005). doi: 10.1021/cr030726o; [PubMed: 15941206]
39. Gaggioli CA, Stoneburner SJ, Cramer CJ, Gagliardi L, Beyond Density Functional Theory: The Multiconfigurational Approach To Model Heterogeneous Catalysis. *ACS Catal.* 9, 8481–8502 (2019). doi: 10.1021/acscatal.9b01775
40. Schlexer Lamoureux P et al., Machine Learning for Computational Heterogeneous Catalysis. *ChemCatChem* 11, 3581–3601 (2019). doi: 10.1002/cctc.201900595
41. Janet JP, Ramesh S, Duan C, Kulik HJ, Accurate Multiobjective Design in a Space of Millions of Transition Metal Complexes with Neural-Network-Driven Efficient Global Optimization. *ACS Cent. Sci* 6, 513–524 (2020).doi: 10.1021/acscentsci.0c00026; [PubMed: 32342001]
42. Meyer B, Sawatlon B, Heinen S, von Lilienfeld OA, Corminboeuf C, Machine learning meets volcano plots: Computational discovery of cross-coupling catalysts. *Chem. Sci* 9, 7069–7077 (2018). doi: 10.1039/C8SC01949E; [PubMed: 30310627]
43. Ulissi ZW et al., Machine-Learning Methods Enable Exhaustive Searches for Active Bimetallic Facets and Reveal Active Site Motifs for CO₂ Reduction. *ACS Catal.* 7, 6600–6608 (2017). doi: 10.1021/acscatal.7b01648
44. Zhong M et al., Accelerated discovery of CO₂ electrocatalysts using active machine learning. *Nature* 581, 178–183 (2020). doi: 10.1038/s41586-020-2242-8; [PubMed: 32405017]
45. Saravanan K, Kitchin JR, von Lilienfeld OA, Keith JA, Alchemical Predictions for Computational Catalysis: Potential and Limitations. *J. Phys. Chem. Lett* 8, 5002–5007 (2017). doi: 10.1021/acs.jpclett.7b01974; [PubMed: 28938798]
46. Bligaard T et al., Toward Benchmarking in Catalysis Science: Best Practices, Challenges, and Opportunities. *ACS Catal.* 6, 2590–2602 (2016). doi: 10.1021/acscatal.6b00183
47. Khersonsky O, Tawfik DS, Enzyme promiscuity: A mechanistic and evolutionary perspective. *Annu. Rev. Biochem* 79, 471–505 (2010). doi: 10.1146/annurevbiochem-030409-143718; [PubMed: 20235827]
48. Davies HML, Morton D, Guiding principles for site selective and stereoselective intermolecular C–H functionalization by donor/acceptor rhodium carbenes. *Chem. Soc. Rev* 40, 1857–1869 (2011). doi: 10.1039/c0cs00217h; [PubMed: 21359404]
49. Brandenburg OF, Chen K, Arnold FH, Directed Evolution of a Cytochrome P450 Carbene Transferase for Selective Functionalization of Cyclic Compounds. *J. Am. Chem. Soc* 141, 8989–8995 (2019). doi: 10.1021/jacs.9b02931; [PubMed: 31070908]
50. Zhang RK et al., Enzymatic assembly of carbon-carbon bonds via iron-catalysed sp³ C–H functionalization. *Nature* 565, 67–72 (2019). doi: 10.1038/s41586-018-0808-5; [PubMed: 30568304]
51. Hartwig JF, Larsen MA, Undirected, Homogeneous C–H Bond Functionalization: Challenges and Opportunities. *ACS Cent. Sci* 2, 281–292 (2016). doi: 10.1021/acscentsci.6b00032; [PubMed: 27294201]
52. Brandenburg OF, Fasan R, Arnold FH, Exploiting and engineering hemoproteins for abiological carbene and nitrene transfer reactions. *Curr. Opin. Biotechnol* 47, 102–111 (2017). doi: 10.1016/j.copbio.2017.06.005; [PubMed: 28711855]
53. Jiménez-Osés G et al., The role of distant mutations and allosteric regulation on LovD active site dynamics. *Nat. Chem. Biol* 10, 431–436 (2014). doi: 10.1038/nchembio.1503; [PubMed: 24727900]

54. Niehaus F, Bertoldo C, Kähler M, Antranikian G, Extremophiles as a source of novel enzymes for industrial application. *Appl. Microbiol. Biotechnol* 51, 711–729 (1999). doi: 10.1007/s002530051456; [PubMed: 10422220]
55. Klibanov AM, Improving enzymes by using them in organic solvents. *Nature* 409, 241–246 (2001). doi: 10.1038/35051719; [PubMed: 11196652]
56. Noyori R, Asymmetric catalysis: Science and opportunities (Nobel lecture). *Angew. Chem. Int. Ed* 41, 2008–2022 (2002). doi: 10.1002/1521-3773(20020617)41:12<2008:AIDANIE2008>3.0.CO;2-4;
57. Zuo W, Lough AJ, Li YF, Morris RH, Amine(imine) diphosphine iron catalysts for asymmetric transfer hydrogenation of ketones and imines. *Science* 342, 1080–1083 (2013). doi: 10.1126/science.1244466; [PubMed: 24288329]
58. Friedfeld MR, Zhong H, Ruck RT, Shevlin M, Chirik PJ, Cobalt-catalyzed asymmetric hydrogenation of enamides enabled by single-electron reduction. *Science* 360, 888–893 (2018). doi: 10.1126/science.aar6117; [PubMed: 29798879]
59. Kiernicki JJ, Zeller M, Szymczak NK, Hydrazine Capture and N-N Bond Cleavage at Iron Enabled by Flexible Appended Lewis Acids. *J. Am. Chem. Soc* 139, 18194–18197 (2017). doi: 10.1021/jacs.7b11465; [PubMed: 29227655]
60. Azcarate I, Costentin C, Robert M, Savéant J-M, Through-Space Charge Interaction Substituent Effects in Molecular Catalysis Leading to the Design of the Most Efficient Catalyst of CO₂-to-CO Electrochemical Conversion. *J. Am. Chem. Soc* 138, 16639–16644 (2016). doi: 10.1021/jacs.6b07014; [PubMed: 27976580]
61. Chantarojsiri T, Ziller JW, Yang JY, Incorporation of redox-inactive cations promotes iron catalyzed aerobic C-H oxidation at mild potentials. *Chem. Sci* 9, 2567–2574 (2018). doi: 10.1039/C7SC04486K; [PubMed: 29732136]
62. Martin DJ, Mercado BQ, Mayer JM, Combining scaling relationships overcomes rate versus overpotential trade-offs in O₂ molecular electrocatalysis. *Sci. Adv* 6, eaaz3318 (2020). doi: 10.1126/sciadv.aaz3318; [PubMed: 32201730]
63. Ford CL, Park YJ, Matson EM, Gordon Z, Fout AR, A bioinspired iron catalyst for nitrate and perchlorate reduction. *Science* 354, 741–743 (2016). doi: 10.1126/science.aah6886; [PubMed: 27846604]
64. Klug CM, Cardenas A, Bullock RM, O'Hagan M, Wiedner ES, Reversing the Tradeoff Between Rate and Overpotential in Molecular Electrocatalysts for H₂ Production. *ACS Catal.* 8, 3286–3296 (2018). doi: 10.1021/acscatal.7b04379
65. Le Goff A et al., From hydrogenases to noble metal-free catalytic nanomaterials for H₂ production and uptake. *Science* 326, 1384–1387 (2009). doi: 10.1126/science.1179773; [PubMed: 19965754]
66. Huan TN et al., Biol.-inspired noble metal-free nanomaterials approaching platinum performances for H₂ evolution and uptake. *Energy Environ. Sci* 9, 940–947 (2016). doi: 10.1039/C5EE02739J
67. Hsu C-W, Rathnayaka SC, Islam SM, MacMillan SN, Mankad NP, N₂O Reductase Activity of a [Cu₄S] Cluster in the 4Cu^I Redox State Modulated by Hydrogen Bond Donors and Proton Relays in the Secondary Coordination Sphere. *Angew. Chem. Int. Ed* 59, 627–631 (2020). doi: 10.1002/anie.201906327;
68. Liu T, Dubois DL, Bullock RM, An iron complex with pendent amines as a molecular electrocatalyst for oxidation of hydrogen. *Nat. Chem* 5, 228–233 (2013). doi: 10.1038/nchem.1571; [PubMed: 23422565]
69. Martin DJ, Mercado BQ, Mayer JM, Combining scaling relationships overcomes rate versus overpotential trade-offs in O₂ molecular electrocatalysis. *Sci. Adv* 6, eaaz3318 (2020). doi: 10.1126/sciadv.aaz3318 [PubMed: 32201730]
70. Warren JJ, Tronic TA, Mayer JM, Thermochemistry of proton-coupled electron transfer reagents and its implications. *Chem. Rev* 110, 6961–7001 (2010). doi: 10.1021/cr100085k; [PubMed: 20925411]
71. Weinberg DR et al., Proton-coupled electron transfer. *Chem. Rev* 112, 4016–4093 (2012). doi: 10.1021/cr200177j; [PubMed: 22702235]

72. Horvath S, Fernandez LE, Soudackov AV, Hammes-Schiffer S, Insights into proton-coupled electron transfer mechanisms of electrocatalytic H₂ oxidation and production. *Proc. Natl. Acad. Sci. U.S.A* 109, 15663–15668 (2012). doi: 10.1073/pnas.1118333109; [PubMed: 22529352]
73. Fried SD, Bagchi S, Boxer SG, Extreme electric fields power catalysis in the active site of ketosteroid isomerase. *Science* 346, 1510–1514 (2014). doi: 10.1126/science.1259802; [PubMed: 25525245]
74. Wang Q, Astruc D, State of the Art and Prospects in Metal-Organic Framework (MOF)-Based and MOF-Derived Nanocatalysis. *Chem. Rev* 120, 1438–1511 (2020).doi: 10.1021/acs.chemrev.9b00223; [PubMed: 31246430]
75. Feng X et al., Metal-Organic Frameworks Significantly Enhance Photocatalytic Hydrogen Evolution and CO₂ Reduction with Earth-Abundant Copper Photosensitizers. *J. Am. Chem. Soc* 142, 690–695 (2020). doi: 10.1021/jacs.9b12229; [PubMed: 31895984]
76. Liu J et al., Introducing Nonstructural Ligands to Zirconia-like Metal-Organic Framework Nodes To Tune the Activity of Node-Supported Nickel Catalysts for Ethylene Hydrogenation. *ACS Catal* 9, 3198–3207 (2019). doi: 10.1021/acscatal.8b04828
77. Otake KI et al., Single-Atom-Based Vanadium Oxide Catalysts Supported on Metal-Organic Frameworks: Selective Alcohol Oxidation and Structure-Activity Relationship. *J. Am. Chem. Soc* 140, 8652–8656 (2018). doi: 10.1021/jacs.8b05107; [PubMed: 29950097]
78. Sun C, Skorupskii G, Dou J-H, Wright AM, Dinc M, Reversible Metalation and Catalysis with a Scorpionate-like Metallo-ligand in a Metal-Organic Framework. *J. Am. Chem. Soc* 140, 17394–17398 (2018). doi: 10.1021/jacs.8b11085; [PubMed: 30497263]
79. Zhang T, Manna K, Lin W, Metal-Organic Frameworks Stabilize Solution-Inaccessible Cobalt Catalysts for Highly Efficient Broad-Scope Organic Transformations. *J. Am. Chem. Soc* 138, 3241–3249 (2016). doi: 10.1021/jacs.6b00849; [PubMed: 26864496]
80. Beyzavi MH et al., A Hafnium-Based Metal-Organic Framework as a Nature-Inspired Tandem Reaction Catalyst. *J. Am. Chem. Soc* 137, 13624–13631 (2015). doi: 10.1021/jacs.5b08440; [PubMed: 26434603]
81. Baek J et al., Bioinspired Metal-Organic Framework Catalysts for Selective Methane Oxidation to Methanol. *J. Am. Chem. Soc* 140, 18208–18216 (2018). doi: 10.1021/jacs.8b11525; [PubMed: 30525562]
82. van Leest NP et al., Single-Electron Elementary Steps in Homogeneous Organometallic Catalysis. *Adv. Organomet. Chem* 70, 71–180 (2018). doi: 10.1016/bs.adomc.2018.07.002;
83. te Grotenhuis C, van den Heuvel N, van der Vlugt JJ, de Bruin B, Catalytic Dibenzocyclooctene Synthesis via Cobalt(III)-Carbene Radical and ortho-Quinodimethane Intermediates. *Angew. Chem. Int. Ed* 57, 140–145 (2018). doi: 10.1002/anie.201711028;
84. Yao C, Dahmen T, Gansäuer A, Norton J, Anti-Markovnikov alcohols via epoxide hydrogenation through cooperative catalysis. *Science* 364, 764–767 (2019). doi: 10.1126/science.aaw3913; [PubMed: 31123133]
85. Chaudhuri P, Hess M, Flörke U, Wieghardt K, From Structural Models of Galactose Oxidase to Homogeneous Catalysis: Efficient Aerobic Oxidation of Alcohols. *Angew. Chem. Int. Ed* 37, 2217–2220 (1998). doi: 10.1002/(SICI)1521-3773(19980904)37:16<2217:AID-ANIE2217>3.0.CO;2-D;
86. Chirik PJ, Wieghardt K, Radical ligands confer nobility on base-metal catalysts. *Science* 327, 794–795 (2010).doi: 10.1126/science.1183281; [PubMed: 20150476]
87. Praneeth VKK, Ringenberg MR, Ward TR, Redox-active ligands in catalysis. *Angew. Chem. Int. Ed* 51, 10228–10234 (2012). doi: 10.1002/anie.201204100;
88. Lyaskovskyy V, de Bruin B, Redox Non-Innocent Ligands: Versatile New Tools to Control Catalytic Reactions. *ACS Catal* 2, 270–279 (2012). doi: 10.1021/cs200660v
89. Darmon JM et al., Oxidative addition of carbon-carbon bonds with a redox-active bis(imino)pyridine iron complex. *J. Am. Chem. Soc* 134, 17125–17137 (2012). doi: 10.1021/ja306526d; [PubMed: 23043331]
90. Zhou Y-Y, Uyeda C, Catalytic reductive [4 + 1]-cycloadditions of vinylidenes and dienes. *Science* 363, 857–862 (2019).doi: 10.1126/science.aau0364; [PubMed: 30792299]

91. Que L Jr., W. B. Tolman, Biologically inspired oxidation catalysis. *Nature* 455, 333–340 (2008). doi: 10.1038/nature07371; [PubMed: 18800132]
92. Carsch KM et al., Synthesis of a copper-supported triplet nitrene complex pertinent to copper-catalyzed amination. *Science* 365, 1138–1143 (2019). doi: 10.1126/science.aax4423; [PubMed: 31515388]
93. Römelt C et al., Electronic Structure of a Formal Iron(0) Porphyrin Complex Relevant to CO₂ Reduction. *Inorg. Chem* 56, 4746–4751 (2017). doi: 10.1021/acs.inorgchem.7b00401; [PubMed: 28379689]
94. Kaminsky CJ, Wright J, Surendranath Y, Graphite-Conjugation Enhances Porphyrin Electrocatalysis. *ACS Catal.* 9, 3667–3671 (2019). doi: 10.1021/acscatal.9b00404
95. Loewen ND, Neelakantan TV, Berben LA, Renewable Formate from C-H Bond Formation with CO₂: Using Iron Carbonyl Clusters as Electrocatalysts. *Acc. Chem. Res* 50, 2362–2370 (2017). doi: 10.1021/acs.accounts.7b00302; [PubMed: 28836757]
96. Ferreira RB, Murray LJ, Cyclophanes as Platforms for Reactive Multimetallic Complexes. *Acc. Chem. Res* 52, 447–455 (2019). doi: 10.1021/acs.accounts.8b00559; [PubMed: 30668108]
97. Nakajima T et al., Synergistic Cu₂ Catalysts for Formic Acid Dehydrogenation. *J. Am. Chem. Soc* 141, 8732–8736 (2019). doi: 10.1021/jacs.9b03532; [PubMed: 31083993]
98. Dey S et al., Electrocatalytic O₂ reduction by [Fe-Fe]-hydrogenase active site models. *J. Am. Chem. Soc* 136, 8847–8850 (2014). doi: 10.1021/ja5021684; [PubMed: 24846692]
99. Sharma S, Sivalingam K, Neese F, Chan GK-L, Low-energy spectrum of iron-sulfur clusters directly from many-particle quantum mechanics. *Nat. Chem* 6, 927–933 (2014). doi: 10.1038/nchem.2041; [PubMed: 25242489]
100. Gagliardi L et al., Multiconfiguration Pair-Density Functional Theory: A New Way To Treat Strongly Correlated Systems. *Acc. Chem. Res* 50, 66–73 (2017). doi: 10.1021/acs.accounts.6b00471; [PubMed: 28001359]
101. Ott JC, Wadepohl H, Enders M, Gade LH, Taking Solution Proton NMR to Its Extreme: Prediction and Detection of a Hydride Resonance in an Intermediate-Spin Iron Complex. *J. Am. Chem. Soc* 140, 17413–17417 (2018). doi: 10.1021/jacs.8b11330; [PubMed: 30486649]
102. Holland PL, Distinctive Reaction Pathways at Base Metals in High-Spin Organometallic Catalysts. *Acc. Chem. Res* 48, 1696–1702 (2015). doi: 10.1021/acs.accounts.5b00036; [PubMed: 25989357]
103. Crockett MP, Zhang H, Thomas CM, Byers JA, Adding diffusion ordered NMR spectroscopy (DOSY) to the arsenal for characterizing paramagnetic complexes. *Chem. Commun* 55, 14426–14429 (2019). doi: 10.1039/C9CC08229H;
104. Lu Q et al., Highly porous non-precious bimetallic electrocatalysts for efficient hydrogen evolution. *Nat. Commun* 6, 6567 (2015). doi: 10.1038/ncomms7567; [PubMed: 25910892]
105. Zhang B et al., Homogeneously dispersed multimetal oxygen-evolving catalysts. *Science* 352, 333–337 (2016). doi: 10.1126/science.aaf1525; [PubMed: 27013427]
106. Trotochaud L, Young SL, Ranney JK, Boettcher SW, Nickel-iron oxyhydroxide oxygen-evolution electrocatalysts: The role of intentional and incidental iron incorporation. *J. Am. Chem. Soc* 136, 6744–6753 (2014). doi: 10.1021/ja502379c; [PubMed: 24779732]
107. Carter EA, Challenges in modeling materials properties without experimental input. *Science* 321, 800–803 (2008). doi: 10.1126/science.1158009; [PubMed: 18687955]
108. Jaramillo TF et al., Identification of active edge sites for electrochemical H₂ evolution from MoS₂ nanocatalysts. *Science* 317, 100–102 (2007). doi: 10.1126/science.1141483; [PubMed: 17615351]
109. Seh ZW et al., Combining theory and experiment in electrocatalysis: Insights into materials design. *Science* 355, eaad4998 (2017). doi: 10.1126/science.aad4998; [PubMed: 28082532]
110. Chen JG, Carbide and Nitride Overlayers on Early Transition Metal Surfaces: Preparation, Characterization, and Reactivities. *Chem. Rev* 96, 1477–1498 (1996). doi: 10.1021/cr950232u; [PubMed: 11848799]
111. Seh ZW et al., Two-Dimensional Molybdenum Carbide (MXene) as an Efficient Electrocatalyst for Hydrogen Evolution. *ACS Energy Lett.* 1, 589–594 (2016). doi: 10.1021/acsenerylett.6b00247

112. Kibsgaard J et al., Designing an improved transition metal phosphide catalyst for hydrogen evolution using experimental and theoretical trends. *Energy Environ. Sci* 8, 3022–3029 (2015). doi: 10.1039/C5EE02179K
113. Levy RB, Boudart M, Platinum-like behavior of tungsten carbide in surface catalysis. *Science* 181, 547–549 (1973). doi: 10.1126/science.181.4099.547; [PubMed: 17777803]
114. Lin Z, Chen R, Qu Z, Chen JG, Hydrodeoxygenation of biomass-derived oxygenates over metal carbides: From model surfaces to powder catalysts. *Green Chem.* 20, 2679–2696 (2018). doi: 10.1039/C8GC00239H
115. Yan B et al., Surface Restructuring of Nickel Sulfide Generates Optimally Coordinated Active Sites for Oxygen Reduction Catalysis. *Joule* 1, 600–612 (2017). doi: 10.1016/j.joule.2017.08.020
116. Dou J et al., Operando chemistry of catalyst surfaces during catalysis. *Chem. Soc. Rev* 46, 2001–2027 (2017). doi: 10.1039/C6CS00931J; [PubMed: 28358410]
117. Wu G, Zelenay P, Nanostructured nonprecious metal catalysts for oxygen reduction reaction. *Acc. Chem. Res* 46, 1878–1889 (2013). doi: 10.1021/ar400011z; [PubMed: 23815084]
118. Zhu YP, Guo C, Zheng Y, Qiao S-Z, Surface and Interface Engineering of Noble-Metal-Free Electrocatalysts for Efficient Energy Conversion Processes. *Acc. Chem. Res* 50, 915–923 (2017). doi: 10.1021/acs.accounts.6b00635; [PubMed: 28205437]
119. Asset T, Atanassov P, Iron-Nitrogen-Carbon Catalysts for Proton Exchange Membrane Fuel Cells. *Joule* 4, 33–44 (2020). doi: 10.1016/j.joule.2019.12.002
120. Pelletier JDA, Basset J-M, Catalysis by Design: Well-Defined Single-Site Heterogeneous Catalysts. *Acc. Chem. Res* 49, 664–677 (2016). doi: 10.1021/acs.accounts.5b00518; [PubMed: 26959689]
121. Nitopi S et al., Progress and Perspectives of Electrochemical CO₂ Reduction on Copper in Aqueous Electrolyte. *Chem. Rev* 119, 7610–7672 (2019). doi: 10.1021/acs.chemrev.8b00705; [PubMed: 31117420]
122. Surendranath Y, Lutterman DA, Liu Y, Nocera DG, Nucleation, growth, and repair of a cobalt-based oxygen evolving catalyst. *J. Am. Chem. Soc* 134, 6326–6336 (2012). doi: 10.1021/ja3000084; [PubMed: 22394103]
123. Marinkovic JM, Riisager A, Franke R, Wasserscheid P, Haumann M, Fifteen Years of Supported Ionic Liquid Phase-Catalyzed Hydroformylation: Material and Process Developments. *Ind. Eng. Chem. Res* 58, 2409–2420 (2019). doi: 10.1021/acs.iecr.8b04010
124. Falsig H et al., Trends in the catalytic CO oxidation activity of nanoparticles. *Angew. Chem. Int. Ed* 47, 4835–4839 (2008). doi: 10.1002/anie.200801479;
125. Solis BH, Maher AG, Dogutan DK, Nocera DG, Hammes-Schiffer S, Nickel phlorin intermediate formed by proton-coupled electron transfer in hydrogen evolution mechanism. *Proc. Natl. Acad. Sci. U.S.A* 113, 485–492 (2016). doi: 10.1073/pnas.1521834112; [PubMed: 26655344]
126. Horike S, Dinc M, Tamaki K, Long JR, Size-selective Lewis acid catalysis in a microporous metal-organic framework with exposed Mn²⁺ coordination sites. *J. Am. Chem. Soc* 130, 5854–5855 (2008). doi: 10.1021/ja800669j; [PubMed: 18399629]
127. Jaouen F et al., Recent advances in non-precious metal catalysis for oxygen-reduction reaction in polymer electrolyte fuel cells. *Energy Environ. Sci* 4, 114–130 (2011). doi: 10.1039/C0EE00011F
128. Kas R et al., Electrochemical CO₂ reduction on nanostructured metal electrodes: Fact or defect? *Chem. Sci* 11, 1738–1749 (2020). doi: 10.1039/C9SC05375A

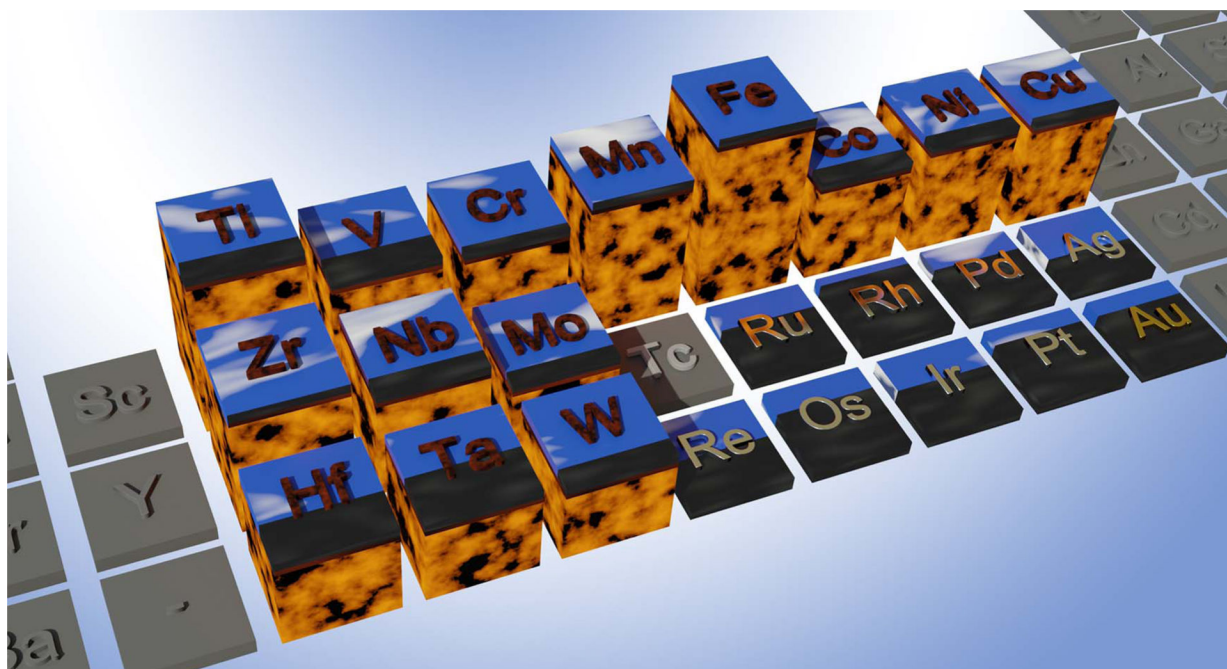
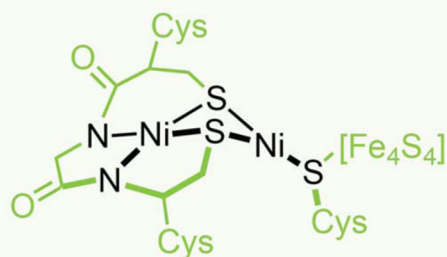
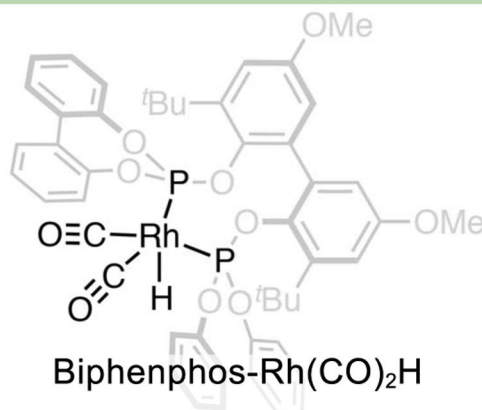
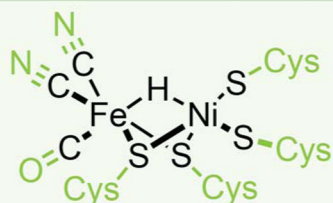


Fig. 1. Definition of different groups of transition metals.

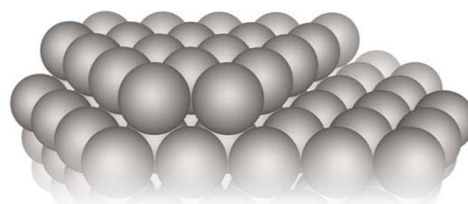
Platinum group metals (PGMs) include Ru, Rh, Pd, Os, Ir, and Pt. The broader term, precious metals, includes PGMs along with Re, Au, and Ag. Earth-abundant metals (EAMs), sometimes referred to as base metals, include all other transition metals. (Tc is shown but is radioactive and unstable.) The height of the pillar for each metal indicates its crustal abundance on a log scale; the values range from 5.6% (Fe) to ~0.001 ppm (Rh, Ir). The black bar on each metal shows (also on a log scale) the relative amount of CO₂ produced through mining and purification for each metal (20), which is markedly larger for PGMs than for EAMs.

Nature's catalysts**Platinum group metal catalysts****Hydroformylation**

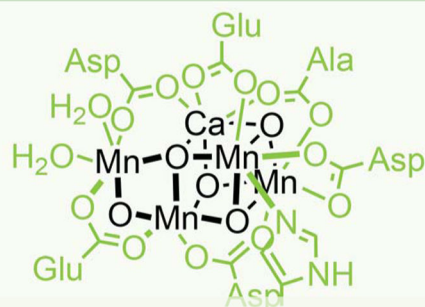
Acetyl-CoA synthase

Biphosphor-Rh(CO)₂H**Hydrogen oxidation reaction**

[NiFe]-Hydrogenase



Pt

Oxygen evolution reaction

Photosystem II

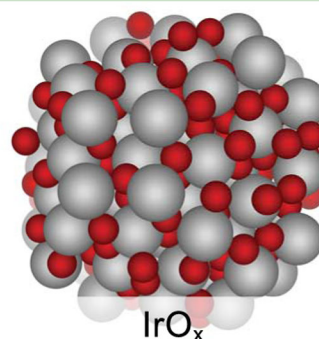
IrO_x

Fig. 2. Many of the transformations carried out by enzymatic EAM catalysts are replicated in the chemical industry by means of PGM catalysts.

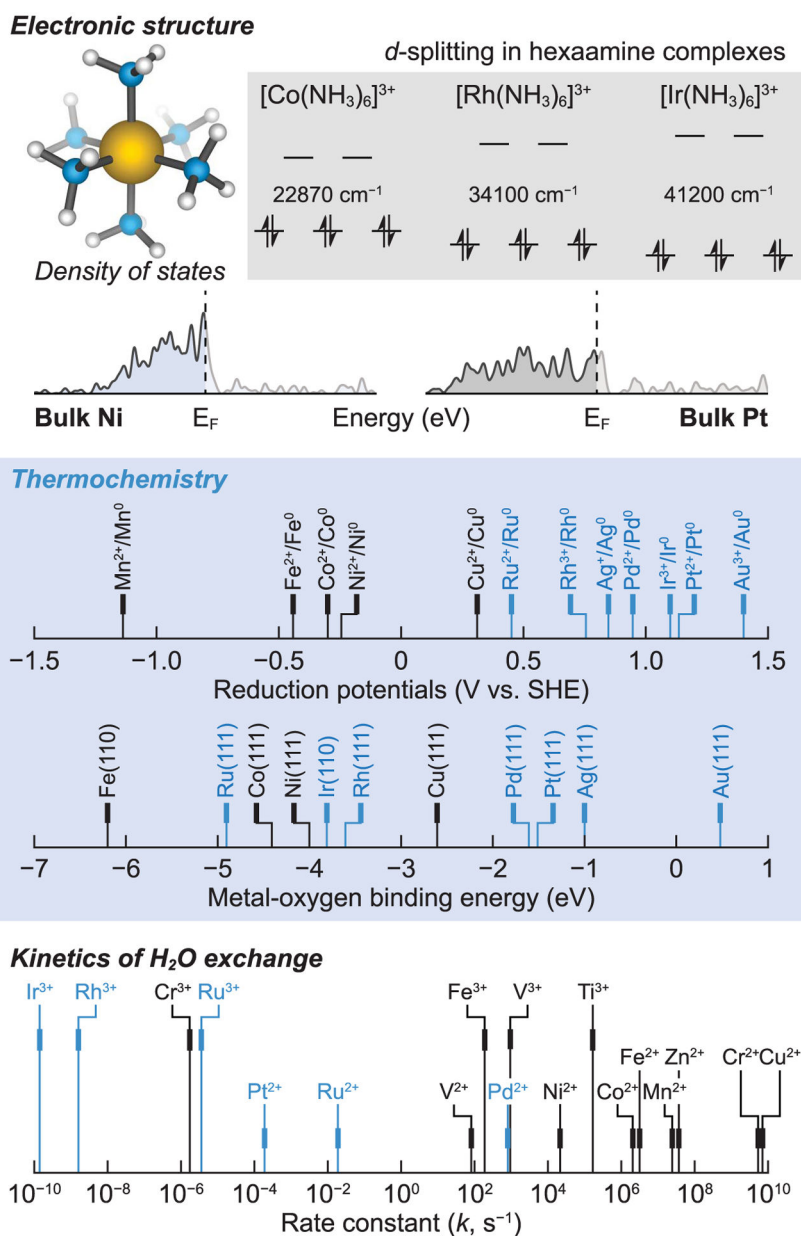
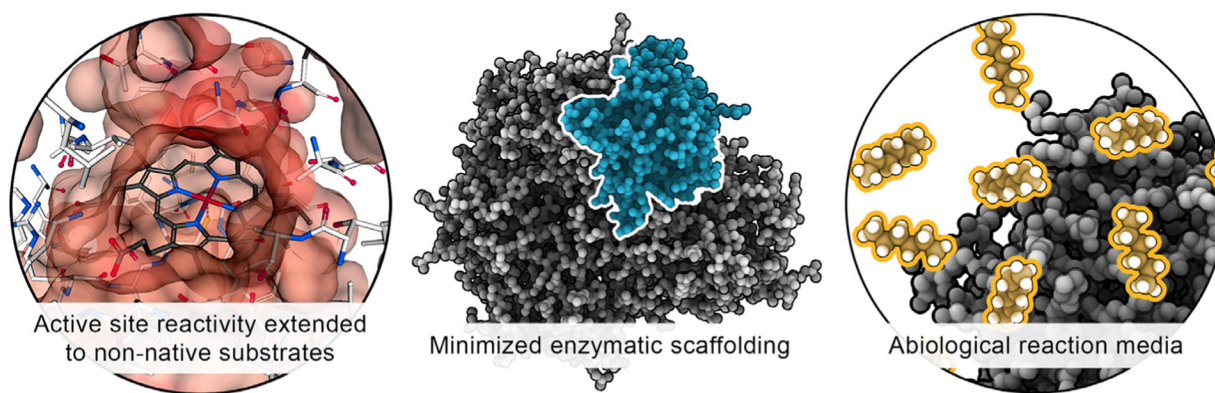


Fig. 3. Physical properties of EAMs versus PGMs, illustrating substantial differences that lead to divergent reactivity that can be exploited in catalysis. Data are from (1, 38, 124).

**Fig. 4.**

The utility of enzymatic catalysis can be enhanced by expanding active-site reactivity to abiotic substrates, minimizing the enzymatic scaffolding, and enabling operation in nonphysiological reaction environments.

Images were obtained from PDB code 1W0E, cytochrome P450.

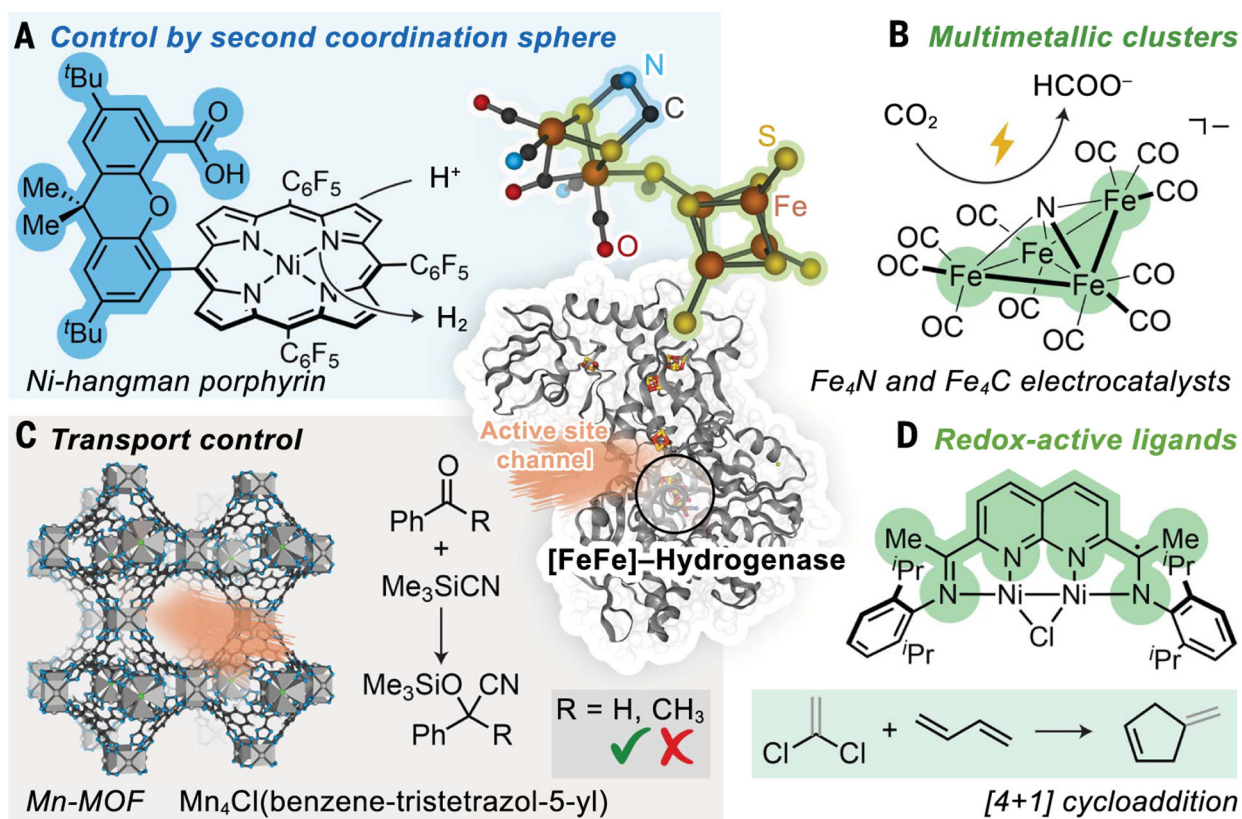


Fig. 5. EAM enzymes provide the blueprint for molecular EAM catalyst design.

The example shown is [Fe-Fe]-hydrogenase (center; PDB code 5LA3). (A) Proton relays positioned proximate to EAM activesites (blue highlight) are deployed in molecular catalysts for hydrogen production (125). (B) Multimetallic cluster active sites catalyze energy conversion reactions (95). (C) Transport to active sites via enzyme channels can be mimicked in porous molecular materials (126). (D) The density of available electronic states is increased through redox-active ligands that can steer reactivity in synthetic systems (90). Me, methyl; *t*Bu, *tert*-butyl; *i*Pr, isopropyl; Ph, phenyl.

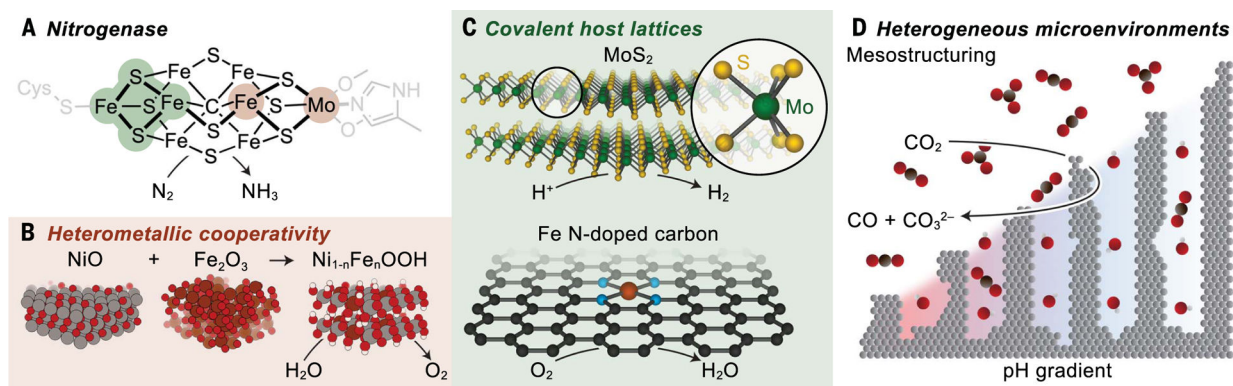


Fig. 6. EAM sites in enzymes such as nitrogenase provide the blueprint for heterogeneous EAM catalyst design.

(A and B) Multimetallic cooperativity in nature [green in (A)] can guide the design of mixed metal-oxide oxygen evolution catalysts (B) (106). (C) The more covalent metal-ligand bonding in natural systems [Fe/Mo in (A)] parallels the more covalent chalcogenide (108) and graphitic carbon host lattices (127) in synthetic catalysts. (D) The function of the fine-tuned catalyst microenvironments in enzymes can be replicated in synthetic catalysts through micro- and mesostructuring (128).